A High-Brightness, Electron-Based Source of Polarized Photons and Neutrons*

J.E. Spencer

Stanford Linear Accelerator Center, Stanford University, Stanford, CA 94309

Abstract. A compact and comparatively inexpensive system that is practical for universities is described based on a low-energy, electron storage ring with at least one undulator based oscillator to store photons. If the oscillator cavity length is relativistically corrected to be an harmonic of the ring circumference ($L_C=\beta L_R n/n_B$ with n_B the number of bunches), higher-energy, secondary photons from Compton backscattering may become significant. Then, besides synchrotron radiation from the ring dipoles and damping wigglers as well as undulator photons, there are frequency upshifted Compton photons and photoneutrons from low Q-value targets such as Beryllium (Q_n=-1.66) or Deuterium (Q_n=-2.22 MeV). For 100 MeV electron bunches, an adjustable-phase, planar, helical undulator can be made to produce circularly polarized UV photons having a fundamental $\varepsilon_{\gamma 1}$=11.1 eV. If these photons are stored in a multimode, hole-coupled resonator they produce a Compton endpoint energy up to $\varepsilon_{\gamma 2}$=1.7 MeV. When incident on a Be conversion target these secondary photons make unmoderated, epithermal neutrons having mean energy ε_n= 24.8±6.8 keV from the two-body reaction $Be^9+\gamma\rightarrow n+Be^8(\rightarrow 2\alpha)$with negligible, residual radioactivity. The system is shown in Fig. 1.

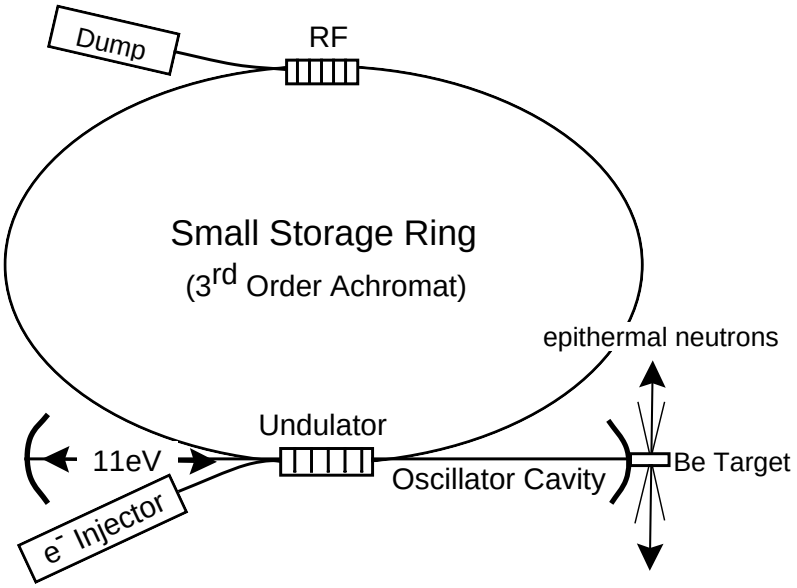

Figure 1. Schematic layout of the basic system when operating with an electron energy of 100 MeV.

When the target is unpolarized, one expects neutron rates of 10^{11} epithermal n/s for 10^{15} Comptons/s and a circulating current of 1 A with polarizations $P_{\mathrm{RHC}}(\vec{n})$=-0.5, $P_{\mathrm{LHC}}(\vec{n})$=0.5, both with reduced flux, and $P_{\mathrm{Lin}}(\vec{n})$=0. With a 1 cm thick cylindrical tungsten sheath surrounding the Be to attenuate scattered photons exiting at 90° to the incident photons, there is a peak neutron flux of $\approx 10^9$ epithermal n/s/cm^2 cylindrically symmetric around the surface. No attempt was made to optimize this because there is still no accepted treatment protocol (dose rates or preferred neutron energy distribution). Although these factors depend on the individual case, several thousand BNCT treatments per year appear feasible. A potential clinical advantage of this system is that it also provides the photon beams required for analogs of NCT such as photon activation therapy PAT. Other medical applications, depending on electron energy, include real-time production of radioactive nuclides (both proton and neutron rich) e.g. tracers for PET scans useful for measuring boron uptake rate and distribution prior to treatment. While the primary electron energy depends on the application, higher energies are more versatile and technically simpler. Certain innovations that make such a system feasible are discussed.

* Funded by Dept. of Energy contract DE-AC03-76SF00515.

Introduction

The method proposed here is quite different from the alternatives for doing NCT discussed in a recent conference(1). Although most of the accelerator based methods have larger neutron production cross sections they appear less efficient for providing the required brightness for a given energy and bandwidth. While many of these may be less expensive, they are more restricted in the problems they can address.

For comparison, the present method provides several alternatives to treat malignant and essentially inoperable tumors that include light-element fission i.e. BNCT using $^{10}B(n,\alpha)Li^7$, heavy-element fission of the actinides using neutrons (n,f) or photons (γ,f) or PAT based on Auger cascades following K-shell ionization by photons. It could also extend the range of photodynamic therapies PDTs.

Non-medical uses for photons include commercial, materials and nuclear science applications up to 2-3 MeV – especially microlithography at 100 nm wavelengths or lower. Practical uses for neutrons include the real-time production of radioactive nuclides and others where there is no direct production of radioactivity e.g. BNCT where there is negligible secondary radioactivity from $^9Be+n\rightarrow Be^{10}\rightarrow{}^{10}B+\beta^-$.

The System

Fig. 1 shows the key components of a system developed in 1995(2). The main element is an electron storage ring with a practical, third-order, achromatic lattice. It is practical because it has minimal multipole families: one dipole, two quad, two sextupole and four octupole – all with modest strengths as shown in Fig. 2.

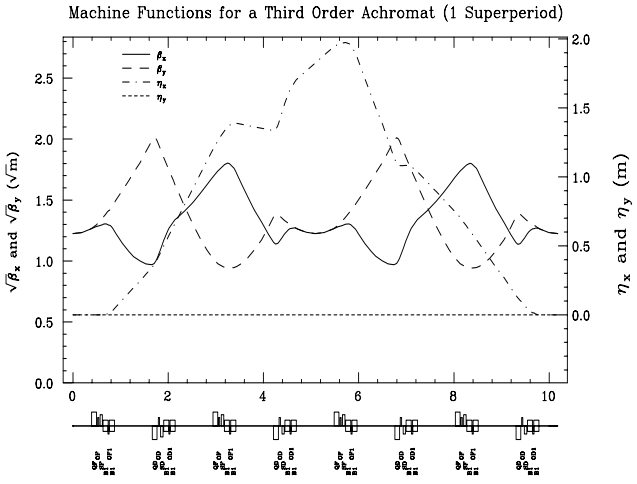

Figure 2. Machine function/magnets for one superperiod.

Of equal practical importance, sufficient dynamic aperture and damping implies the ring can operate as an FEL having significant gain. Large dynamic aperture can be achieved by implementing combined function multipoles using a technique(3) for compact spectrometers and using planar undulators *and* RF structures.

For 100 MeV electrons, an 8.2 mm undulator produces 11.1 eV polarized UV photons. These photons are stored with high efficiency in a cavity formed of multilayer Al, Mg (or Li) mirrors(4) tuned to provide the appropriate Compton endpoint energy. Although such mirrors have not been made, we believe they will be. One alternative is to simply increase the electron energy e.g. if ε_e=200 MeV, we could use a laser with very good, inexpensive mirrors. While increasing the energy would be more expensive, the 'difficulty' costs probably favor it. However, we want the lower energy because it also allows microlithography at $\leq$0.1 μm. Large gains introduce the question of the mirror damage threshold that is a major limiting constraint to be discussed.

Given a lattice, one calculates synchrotron radiation integrals that define the conventional, unperturbed, damping times and emittances(5):

$$\varepsilon_x \approx \frac{1}{2\pi}\frac{c_q\gamma^2}{\rho^2 J_x}\oint_D (\beta_x\eta_x'^2 + 2\alpha_x\eta_x\eta_x' + \gamma_x\eta_x^2)ds$$

where α_x=-β_x'/2 and γ_x=(1+α_x^2)/β_x and the other machine functions are given in Fig. 2. Using H for the argument of the previous integral gives (for 100 MeV electrons):

$$\varepsilon_x \approx 0.234\frac{\varepsilon_e^2[GeV]}{\rho^2}\oint_D H\,ds\ [\mu\text{m}] \ = \ 0.057\ \mu\text{m}$$

because the damping partitions are $J_{x,y,\varepsilon}$=1.005,1,1.995. This emittance is acceptable compared to λ/4 of the UV and for single-turn injection but is easily reduced by lowering η and β in the lattice from their peak values.

Using ε_x=ε_y=0.057 μm for the electron beam with β_x=β_y=1.5 m from Fig. 2 at the insertion waist where η_x=η_y=0 gives equilibrium RMS beam parameters:

$$\sigma_x = \sigma_y = 0.29 \text{ mm}$$
$$\sigma_{x'} = \sigma_{y'} = 0.20 \text{ mrad}$$

in the undulator. By design, these angles are less than the characteristic 1/γ divergence of the radiation to preserve the energy-angle correlation in Compton scattering. While *not* maximized for a minimal spot size in the undulator, they also do not lead to any significant increase in the natural (SR) emittance when there is fast damping.

Beyond the incoherent energy loss from SR, the losses from resistive wall (Cu or glidcop) and parasitic modes are typically only 45 eV/turn giving a combined total of <250 eV/turn/particle ignoring RF inefficiencies, primary (coherent) FEL or secondary, fast Compton damping that is dominant at 26 keV/turn/particle.

The Primary Photon Energy $\varepsilon_{\gamma 1}$ and Intensity

An adjustable-phase, planar, helical undulator makes elliptically polarized photons that can be used to make a Compton endpoint energy $\varepsilon_{\gamma 2}^{max} \equiv \varepsilon_C$=1.7 MeV. The primary undulator photon energy is:

$$\varepsilon_{\gamma 1}(\theta) = \frac{2\gamma^2}{(1+\gamma^2\theta^2+\frac{1}{2}K^2)}(\frac{hc}{\lambda_u})$$

where θ is the radiation angle relative to the undulator axis. The angular dependence is valid for $\sigma_{x'}=\sigma_{y'} \ll 1/\gamma$. Likewise, K defines the maximum angle (K/γ) between the electron's velocity and the undulator axis whenever the rms beam divergences are much smaller:

$$K = eB_u/mck_u = 0.934B_u[T]\lambda_u[cm] .$$

B_u, λ_u and K are related in an energy independent way. The energy of the fundamental at the peak is:

$$\varepsilon_{\gamma 1}^{max}[eV] = \frac{2\gamma^2}{(1+\frac{1}{2}K^2)}(\frac{hc}{\lambda_u}) = \frac{949.6}{(1+\frac{1}{2}K^2)}\frac{\varepsilon_e^2[GeV]}{\lambda_u[cm]}$$

and the photon flux at this energy is

$$\frac{dN_{max}(\varepsilon_{\gamma 1}^{max})}{dt} \approx 1.4\cdot 10^{17}\frac{N_u K^2 I[A]}{(1+\frac{1}{2}K^2)}\frac{\delta\omega}{\omega}$$

where N_u is the number of undulator periods. Note that $N_{max} \to 0$ as K^2 and, although $\varepsilon_{\gamma 1}^{max}$ depends on ε_e, N_{max} does not – in contrast to synchrotron radiation.

For FWHM, $\frac{\delta\omega}{\omega}=1/N_u$ so that $N_u \geq 20$ gives efficient Compton conversion for a neutron threshold ε_{T_n}=1.66 MeV while $N_u=2\beta_{x,y}/\lambda_u \approx 375$ matches the 1.5 m beta function in the undulator for $\varepsilon_{\gamma 1}^{max}$=11.1 eV. Average currents of 1 Amp and K=1 (a reasonable average over the range ε_e=100-200 MeV) give an integrated flux of $\approx 10^{17}$ photons per second produced in the bandwidth of the fundamental that can produce an endpoint energy well above 1.66 MeV. For 75 bunches and 10^7 turns/s this is $2\cdot 10^8$ photons/pass/bunch. With no gain and good mirrors this gives intracavity pulses $N_{\gamma 1} \geq 10^{11}$ at 10 kHz i.e. with ring down times τ_Q=0.1 ms.

The Secondary Photon Energy $\varepsilon_{\gamma 2}$ and Intensity

Ordinary, single-photon Compton scattering for small incident photon angles θ_1 and $\varepsilon_{\gamma 1}$ gives:

$$\varepsilon_{\gamma 2}(\theta_2) = \frac{4\gamma_1^2}{(1+\gamma_1^2\theta_2^2+4\gamma_1\varepsilon_{\gamma 1}/mc^2)}\varepsilon_{\gamma 1} .$$

We can make the correspondence $K_C^2=8\gamma\varepsilon_{\gamma 1}/mc^2 \ll 1$ for most $\varepsilon_1=\varepsilon_e$ and $\varepsilon_{\gamma 1}$:

$$\frac{1}{2}K_C^2 = 0.0153\varepsilon_e[GeV]\varepsilon_{\gamma 1}[eV] \propto \varepsilon_e^3 .$$

For ε_e= 100 MeV, K_C=0.186. $\varepsilon_{\gamma 1}$ can be changed in several ways. The RMS addition to the electron beam's angular divergences ($\sigma_{x'}=\sigma_{y'}$=0.20 mr) from the Compton process is negligible(2) because $\psi_{e2}^{max} < 0.003^\circ \approx 50\ \mu$rad.

For gaussian incident bunches, the luminosity for $(e_1\vec{\gamma}_1 \to e_2\vec{\gamma}_2)$ reactions in terms of the particles in a single electron bunch N_B and the undisrupted, rms spot sizes $\sigma_{x,y}^*$ at the insertion is

$$L = n_c\frac{n_t n_B N_B N_{\gamma 1} H_D}{4\pi\sigma_x^*\sigma_y^*}\zeta \to n_c\frac{I_e(A)}{e}(\frac{N_{\gamma 1}}{4\pi\widehat{\sigma}^2})$$

where n_B is the number of bunches in the ring and n_t is the number of turns/s. $N_{\gamma 1}$ is the number of (incoherent) undulator photons/bunch and n_c is the number of collisions in the cavity a bunch makes in a single pass. The dimensionless parameter H_D defines the effective spot sizes in interaction and the arrow implies round spots:

$$\sigma_{x,y}^* \equiv [\sigma_{x,y}^2+\lambda_{\gamma 1}\lambda_u N_u/(4\pi)^2]^{\frac{1}{2}} \approx \sigma_{x,y} \approx \widehat{\sigma} .$$

$N_{\gamma 1}$ is the effective number of photons per bunch in collision with single pass gain G and mirror efficiency R. For no gain or external sources $\zeta=1/(1-R^2)$. Assuming mirrors with good reflection efficiency(4) R=0.999 and no gain gives $N_{\gamma 1}=10^{11}$. Using n_c=6 in the multimode cavity (photon storage ring) gives $L=3.6\cdot 10^{32}/cm^2s$ showing clearly that gain is required.

A major limit is the $\approx 1 J/cm^2$/pulse mirror damage threshold achievable. For $\varepsilon_{\gamma 1}$=11.1 eV, $\lambda_{\gamma 1}$=112 nm

$$\sigma_{\gamma 1'} = \sqrt{\frac{\lambda_{\gamma 1}}{N_u\lambda_u}} \geq 0.2mr$$

for $N_u \leq 375$ – the matching condition for $\beta_{x,y}$=1.5 m. Using N_u=200 gives an approximate 1 cm^2 spot. An RF frequency of f=750 MHZ (1 MW klystrons are commercially available) allows 75 bunches with $N_{\gamma 1}^{max} \approx 6\cdot 10^{17}$ and $R_{\gamma 2}=1.3\cdot 10^{15}$/s or $R_{\gamma 2}=1.3\cdot 10^{13}\delta_{\gamma 2}(\%)$ where $\delta_{\gamma 2}=\delta\varepsilon_{\gamma 2}/\varepsilon_{\gamma 2}$. This superficially violates the Madey gain-spread theorem because it is possible to provide an external assist, e.g. from the injector or conventional laser(6). Nevertheless, it reinforces the argument for somewhat higher electron energies. Because we can go to higher energies for more damping, more powerful lasers and better mirrors we will use this value for $N_{\gamma 1}$.

Neutron Production

Under our assumptions, we had a secondary photon efficiency $\zeta_{\gamma 2} \leq 0.04/1.7=2.4$ % for the Compton photons capable of producing neutrons of which 0.3 % are expected to make neutrons(7) before Compton scattering or absorption(8) so that $\zeta_n \leq 7.2\cdot 10^{-5}$. This translates into a monochromatic neutron rate $R_n=10^{11}$ n/s with mean energy ε_n=24.8 keV and σ_ε=6.8 keV based on detailed Monte Carlo calculations such as shown in Fig's. 3-4(9).

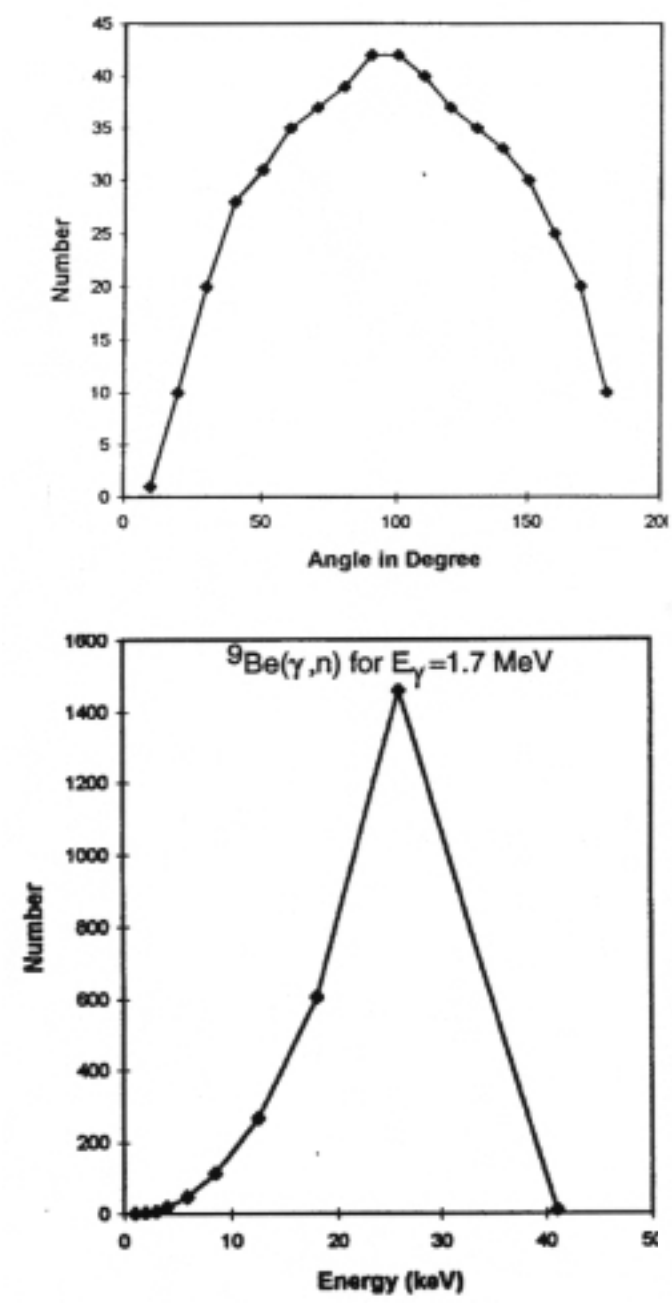

Figure 3. Calculated neutron distributions.

The rate can be improved in a number of ways(6). Furthermore, using an existing ring e.g. PEP-II that is larger and well matched to the conditions with I_e>1 A implies a rate R_n>10^{14} n/s. Finally, C^{13} gives a nominal $P(\vec{n})$=1.0.

REFERENCES

1. The Eight Int'l. Symp. on Neutron Capture Therapy for Cancer, Sept.13-18, 1998, La Jolla, CA.
2. P.L. Morton and J.E. Spencer, Design of an Efficient, Variable Energy, Variable Intensity Photon Beam, NSF Rept. under Contract 9560868, June 12, 1995.
3. J.E. Spencer and H.A. Enge, Split-Pole Spectrograph for Precision Nuclear Spectroscopy, *Nucl. Instrum. Methods***49**, 181 (1967).
4. L.L. Balakireeva, A. Vinogradov and I.V. Kozhevnikov, Optimization of High Reflectivity, Multilayer Mirrors for the Range of 100-150 nm, Kvantovaya Elektron. (Moscow), 20(No.9)(1993)933.
5. R.H. Helm, M.J. Lee, P.L. Morton and M. Sands, Evaluation of Synchrotron Radiation Integrals, *IEEE Trans. Nucl. Sci.***20**, 900 (1973).
6. J.E. Spencer, Efficient, High Brightness Sources of Polarized Neutrons and Photons and Their Uses, SLAC-PUB-7814, 1998.
7. B.L. Berman, R.L. van Hemert and C.D. Bowman, Threshold Photoneutron Cross Section for Be^9, *Phys. Rev.***163**, 958 (1967).
8. Robley D. Evans, *The Atomic Nucleus*, McGraw Hill, New York, 1955.
9. K. Frankel et al., Efficient Source for Cancer Therapy, Eight Int'l. Symp. on Neutron Capture Therapy for Cancer, ibid.

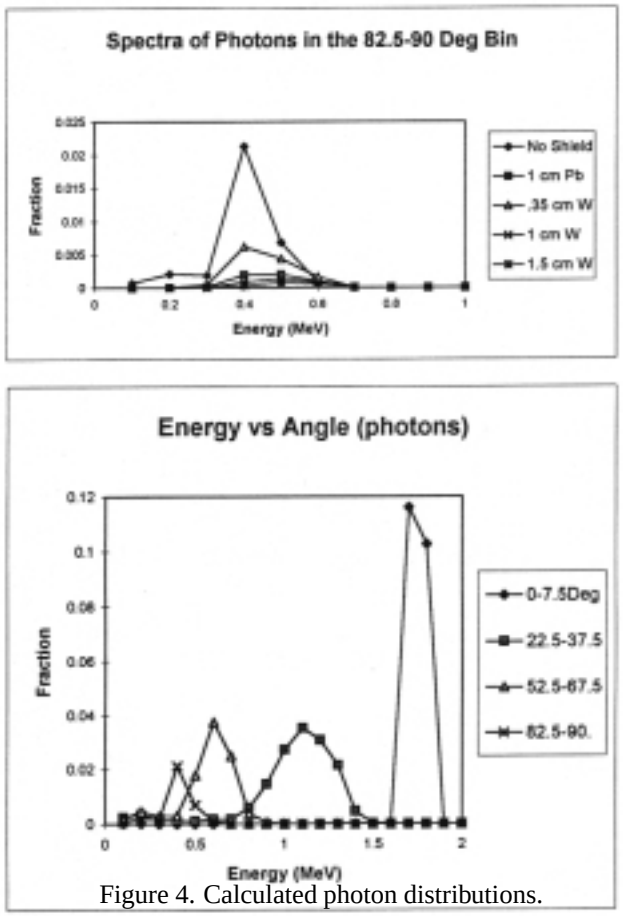

Figure 4. Calculated photon distributions.